

DEPOSITION OF ta-C:N:H AS FUNCTION OF EXPERIMENTAL PARAMETERS

S. E. Rodil and S. Muhl

The incorporation of nitrogen into tetrahedral amorphous carbon films (ta-C:H) was investigated as a function of different gas sources, ion energies and substrate temperatures. Samples were deposited using a highly energetic plasma method: electron cyclotron wave resonance. Composition was measured by nuclear techniques or by XPS. The optical gap was determined by reflection and transmission measurements of samples deposited on quartz substrates and the bonding state was investigated by Raman and infrared (ir) spectroscopy. All the results suggest that tetrahedral bonding is lost, as the nitrogen content increases independently of the deposition parameters used. Structural changes indicated a more polymeric

structure with the formation of $>C=N$, $-C\equiv N$ and $>NH$ groups.

SE/S271

The authors are at IIM-UNAM, Circuito Exterior S/N, CU, Mexico DF 04510, Mexico (ser38@zinalco.iimatercu.unam.mx). Manuscript received 15 August 2003; accepted 9 December 2003.

Keywords: Hydrogenated amorphous carbon, Carbon nitride, Bonding, High density plasma, Optical gap, Hydrocarbon gases, Electron cyclotron wave resonance

© 2004 IoM Communications Ltd. Published by Maney for the Institute of Materials, Minerals and Mining.

INTRODUCTION

The deposition of amorphous carbon containing nitrogen has received particular attention since the theoretical prediction of a metastable phase equivalent to the crystalline phases of silicon nitride, i.e. α - and β - C_3N_4 .^{1,2} According to these predictions, C_3N_4 might exhibit hardness and thermal conductivity values comparable with those of diamond. However, most attempts to synthesise this compound have yielded amorphous material with a nitrogen content lower than expected ($N/C=4/3$) and a low fraction of sp^3 bonded carbon.³ In only a few cases, incomplete evidence for the formation of small crystallites embedded in an amorphous phase has been presented.^{4,5} Nevertheless, there has been considerable effort to synthesise amorphous carbon nitride (a-CN_x) films.⁶ These are known to have interesting tribological properties and can be used as wear resistant films, e.g. for coating magnetic hard disks.

There are four basic types of carbon nitride films. The first type is a-CN_x prepared by reactive sputtering in which carbon is usually sp^2 bonded ($>70\%$), and the nitrogen does not cause significant changes in the state of hybridisation of the carbon.⁷ The second type is ta-CN_x prepared by the filtered cathodic vacuum arc (FCVA).^{8,9} Here, the carbon is mainly sp^3 bonded ($>60\%$), and the addition of nitrogen causes the carbon to become more sp^2 bonded. The third type is a-CN_x:H prepared by conventional plasma enhanced chemical vapour deposition (PECVD) using source gases such as methane and ammonia or nitrogen.¹⁰ In this case, the carbon atoms have a moderate fraction of sp^3 bonds (40–60%), but the network is not particularly dense or highly connected because of the sizeable fraction of hydrogen ($>30\%$.) The fourth type, ta-CN_x:H, can be prepared from a high density plasma source, where the hydrogen content is lower ($\sim 25\%$), and the carbon sp^3 content is higher ($>60\%$).¹¹

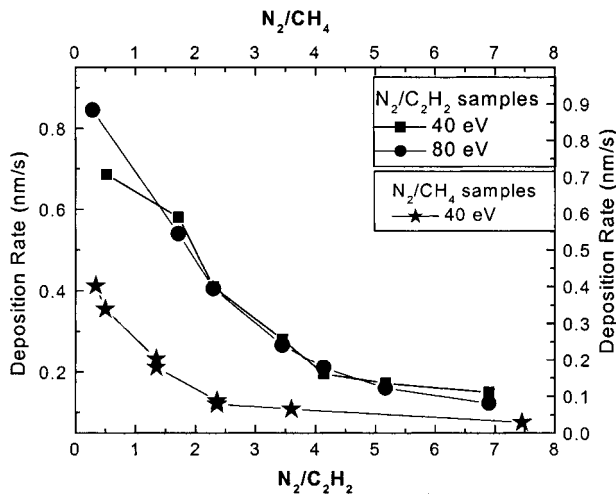
The present paper reports the results of the chemical composition, bonding structure and optical properties of ta-C:N:H films deposited by an

electron cyclotron wave resonance (ECWR) source using N_2/C_2H_2 and N_2/CH_4 plasmas and experimental parameters based on the preparation of good quality tetrahedral amorphous carbon films (ta-C:H), since this might be expected to promote the formation of sp^3 CN bonds.

EXPERIMENT

The ta-C:N:H films were deposited using N_2 and hydrocarbons as the source gases in an ECWR plasma beam source onto silicon $\langle 100 \rangle$ and Corning glass substrates as a function of N_2/C_2H_2 or N_2/CH_4 gas flow ratio $R=0-7$, ion energy 40–110 eV and substrate temperature 30–600°C. The ECWR plasma source comprises a wide single turn electrode surrounded by two Helmholtz coils by which a static transverse magnetic field (~ 12 G) is applied. High plasma densities can be produced by a resonant mechanism established by the interaction between the static magnetic field and the inductively coupled rf current applied to the single turn electrode.¹² The ion energy is controlled by an electrostatic acceleration extraction system, therefore permitting independent control of the ion energy (through variation in the plasma potential) and the ion current density (by rf power and pressure).¹³ The pressure prior to deposition was less than 5×10^{-6} mbar, and during deposition remained below 5×10^{-4} mbar. However, small variations occurred as the nitrogen to hydrocarbon gas ratio was varied from 0 to 7 (the total flow varied between 10 and 30 $smL\ min^{-1}$). A Faraday cup mounted in the substrate holder was used to measure the ion energy and ion current densities. The measured current density varied between 0.35 $mA\ cm^{-2}$ and 0.2 $mA\ cm^{-2}$ as a function of the nitrogen partial pressure owing to the higher ionisation energy of nitrogen (14.6 eV) compared to acetylene (11 eV) or methane (10 eV).

Rutherford backscattering (RBS) and elastic recoil detection analysis (ERDA) were used to determine the nitrogen and hydrogen content, respectively.¹⁴ For the methane samples, the composition was



1 Growth rate against N_2 to C_2H_2 and CH_4 ratios for samples deposited at 40 and 80 eV

determined by XPS analyses carried out with a Thermo Scientific Multilab 2000 using the Al K_{α} line (1486.6 eV). The bonding structure was determined through infrared (ir) spectroscopy (BONEM DA-3) in the range 400–4000 cm^{-1} . A total of 300 scans were used to improve the low signal to noise ratio due to the small thickness of the films. Unpolarised Raman spectra were recorded in backscattering geometry using 514.5 nm excitation from an Ar ion laser and a Jobin-Yvon T64000 triple grating spectrometer. The resolution was about 3 cm^{-1} and care was taken to avoid sample damage during measurements. The sp^2 carbon fraction was determined by electron energy loss spectroscopy (EELS) carried out by STEM in a Vacuum General HB501 microscope with a dedicated parallel EELS spectrometer. The optical gap was derived from transmission and reflection measurements.

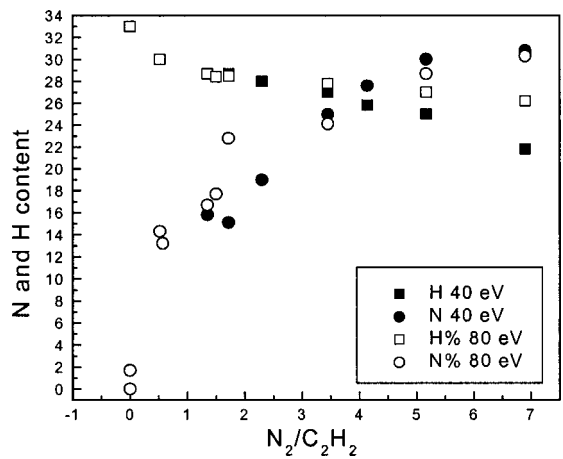
RESULTS AND DISCUSSION

Effect of ion energy

The results in previous papers refer to ta-CHN samples deposited at ion energies of 80 eV.¹⁵ However, the present study is interested in determining the effect of the ion energy on film properties. Therefore, two series of samples were investigated: a series of samples was deposited at the same N_2/C_2H_2 ratios as the previous ta-CHN samples at 80 eV, but using 40 eV. In the second part of the experiment, the N_2/C_2H_2 was fixed at 1.35 and the ion energy was increased from 40 to 110 eV.

Comparison between various N_2/C_2H_2 at 40 and 80 eV

Figure 1 compares the deposition rates as a function of the N_2/C_2H_2 ratio for samples deposited at 40 and 80 eV. Curiously, similar values were obtained for both energies. The decrease in the deposition rate for the two series limits the growth of CN films under high nitrogen partial pressures. The composition (N and H content), as measured by RBS-ERDA, is shown in Fig. 2 as a function of the N_2/C_2H_2 ratio. Both series showed the same trend; the nitrogen content increases rapidly and then saturates to a value ~ 30 at.-%, whereas the hydrogen content gradually

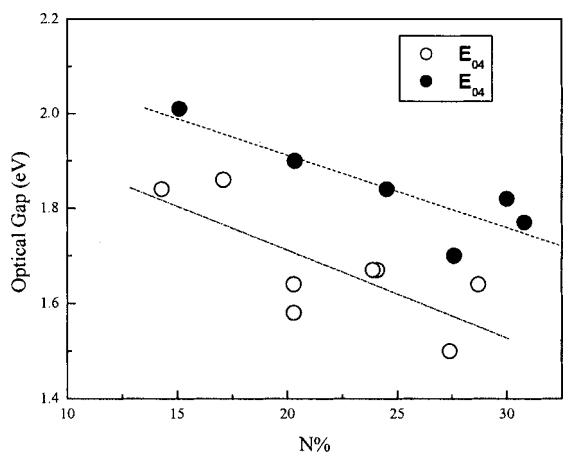


2 Nitrogen and hydrogen content (at.-%) as function of N_2/C_2H_2 ratio for samples deposited at 40 eV

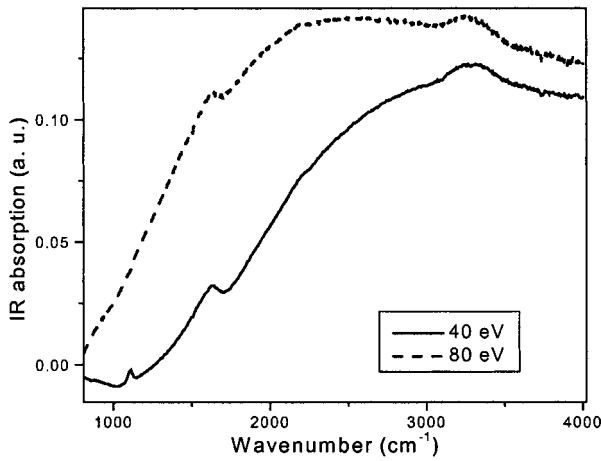
decreases. The combination of the high ionisation of the nitrogen gas and low energy bombardment allows the nitrogen content to attain higher values than those reported by conventional PECVD systems. However, there is also a saturation of the nitrogen content as reported in many other papers and suggested to be due to the formation of N_2 at or below the film surface.

The major difference between the samples is the optical gap that is slightly higher for the 40 eV samples, clearly seen in Fig. 3. This figure shows the E_{04} gap as a function of nitrogen content in the films. This was the first indication of the more polymeric character of the low energy samples.

The ir spectra of the higher nitrogen content samples are shown in Fig. 4 for both series. Unfortunately, a high background due to light dispersion in the rough back surface of the silicon substrate made the comparison of the ir peak intensities very difficult. However, the broad asymmetric band (~ 1000 – 1600 cm^{-1}) and the NH absorption band (3300 cm^{-1}) can be clearly seen above the background, but there is no evidence of CH (< 3000 cm^{-1}) bonding. There is no unique assignment for the 1000 – 1600 cm^{-1} band and, according to the authors' interpretation of the ir spectra of CN films presented in previous papers,^{15,16} it is mainly due to the delocalisation of π electrons among the



3 Variation in E_{04} optical gap as function of nitrogen partial pressure for samples deposited at 40 (●) and 80 eV (○)



4 Infrared spectra of samples prepared using 40 and 80 eV

sp^2 sites, with the corresponding enhancement in ir absorption. The asymmetry at 1600 cm^{-1} is characteristic of hydrogenated samples and, although it is neither a direct CH nor a NH vibration, it could be a C–C vibration enhanced by the presence of hydrogen as a third neighbour. An important characteristic of the 40 eV samples is the higher transparency in the ir region, demonstrated by the appearance of the SiO_2 peak (1100 cm^{-1}), not observed in the 80 eV samples of similar thickness.

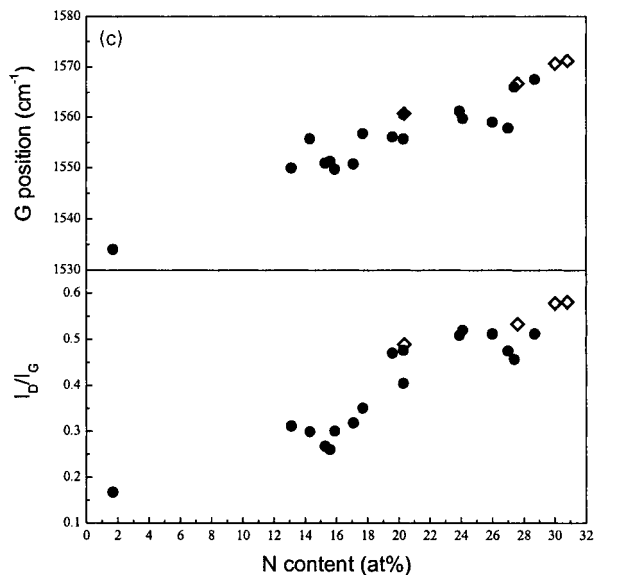
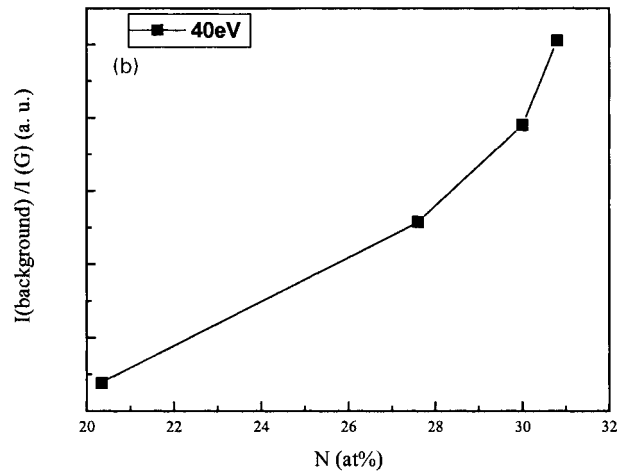
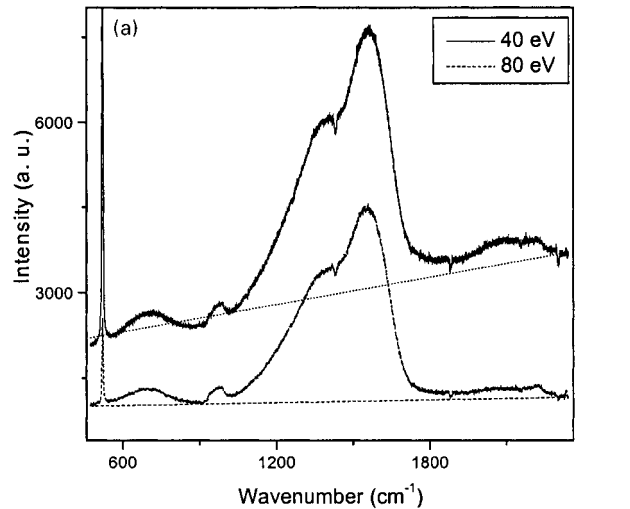
The Raman spectra of the corresponding high nitrogen content samples are shown in Fig. 5a. The main features in the spectra are the G (1568 cm^{-1}) and D (1300 cm^{-1}) peaks and the smaller L peak at 700 cm^{-1} . The only detectable difference was the increase in the background for the 40 eV samples. Figure 5b shows the ratio between the slope of the linear background ($\sim 1880\text{ cm}^{-1}$) and the G intensity as a function of the nitrogen content for the 40 eV sample.

Previous work has shown there is no need for the introduction of new peaks in the Raman spectra of CN films.¹⁷ Therefore the G (due to C–C sp^2 bonds) and D (due to aromatic rings) peaks were fitted simultaneously by a Breit–Wigner–Fano function for the G peak and a Lorentzian for the D peak. The trend in the Raman parameters, G position and $I(D)/I(G)$ are plotted in Fig. 5c as functions of the nitrogen content. Both parameters increase with the nitrogen content, suggesting a nitrogen induced clustering of the sp^2 phase, composed by either aromatic or heteroaromatic rings.

Fixed N_2/C_2H_2 and variable ion energy

The effect of the ion energy on the properties of the films was also investigated by fixing the N_2/C_2H_2 ratio and varying the ion energy. For this series, the films deposited at higher energy contained a lower percentage of hydrogen as shown in Fig. 6a and in good agreement with previous results for ta-C:H films.¹⁸ Consequently, with the percentage decrease in hydrogen, there is an increase in the mass density, as shown in Fig. 6b.

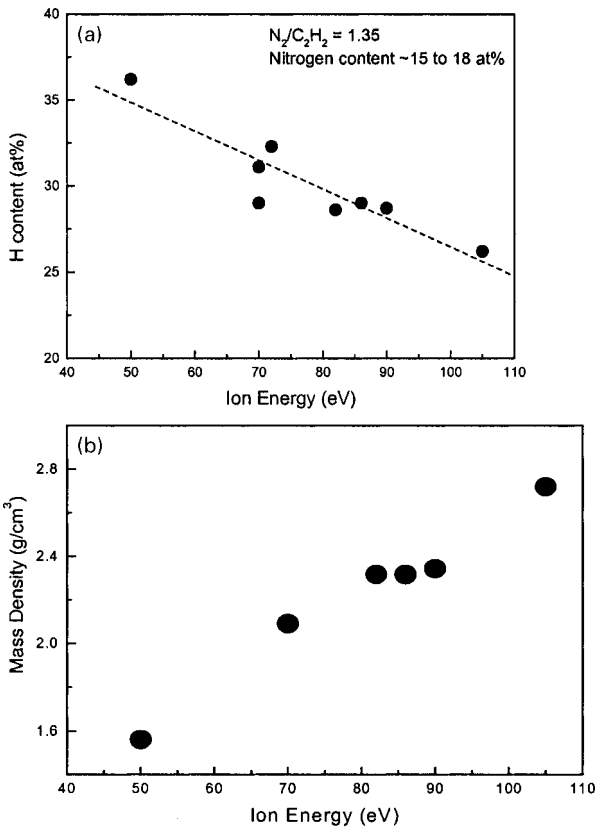
However, the effect of the ion energy on the nitrogen content is not clear. The nitrogen content decreases by only a small amount from 18 to 15 at.-%



5 a Raman spectra for 40 and 80 eV high nitrogen content samples; b background intensity normalised to G peak intensity for 40 eV sample as function of nitrogen content; c G position and $I(D)/I(G)$ intensity ratio as function of nitrogen content

as the ion energy increases, but the values are within experimental error.

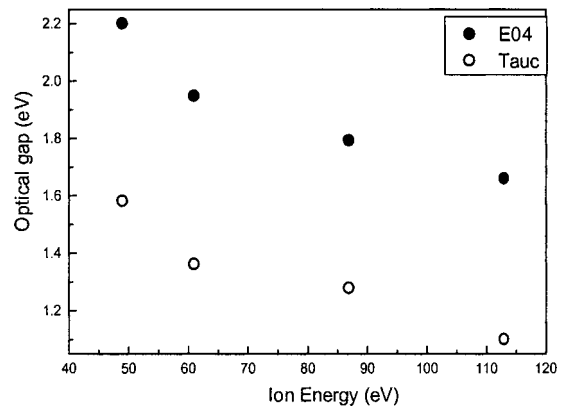
The variation in optical gap with respect to the ion energy is shown in Fig. 7. The optical gap (E_{04}) decreases from 2.2 to 1.6 eV as the ion energy is increased.



6 *a* Hydrogen content as function of ion energy; *b* mass density vs ion energy

Discussion of effect of ion energy

Film properties changed from more polymeric, soft and wide band gap, to diamond-like, hard and lower band gap, as the ion energy increased, in a similar way to that of a-C:H films. The ion energy had its major effect on the hydrogen distribution; sp^2 CH bonds are probably broken, hydrogen is released and new C-C sp^3 bonds are formed. This was confirmed by a small increment detected in the C sp^3 fraction, measured by EELS. However, the lower hydrogen content and its preferential NH bonding allows a higher degree of clustering of the sp^2 phase, with a subsequent decrease in the optical band gap. The more polymeric character of the low energy films is clearly seen by the wide optical gap and the strong photoluminescence background in the Raman spectra. Although no luminescence measurements were made, the background radiation observed in the Raman spectra is known to be due to photoluminescence (PL).¹⁹ This background is usually present in a-C:H films with high hydrogen contents and its enhancement is related to a higher PL intensity. According to Marchon,¹⁹ the ratio between the slope of the fitted linear background and the intensity of the G peak can be used as a measure of the bonded hydrogen content. The larger the ratio, the higher the hydrogen content and also the greater the polymeric character of the films. It should be noted that, in a-C:H films, the PL intensity increases with the hydrogen content. However, for these ta-C:N:H samples, the hydrogen content does not increase. Therefore, the mechanism which enhances the PL intensity in these samples is different from that in a-C:H samples. The enhancement of PL intensity with the increase in nitrogen content in polymeric a-C:N:H films was previously reported



7 E_{04} and Tauc gaps for ta-C:N:H samples against ion energy

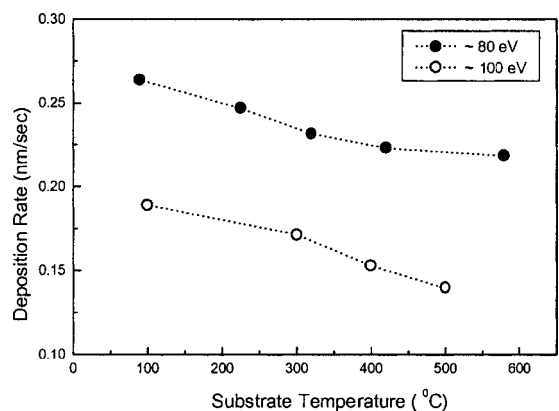
by Mutsukura,³¹ but the origin of this effect is still an open question.

Effect of substrate temperature

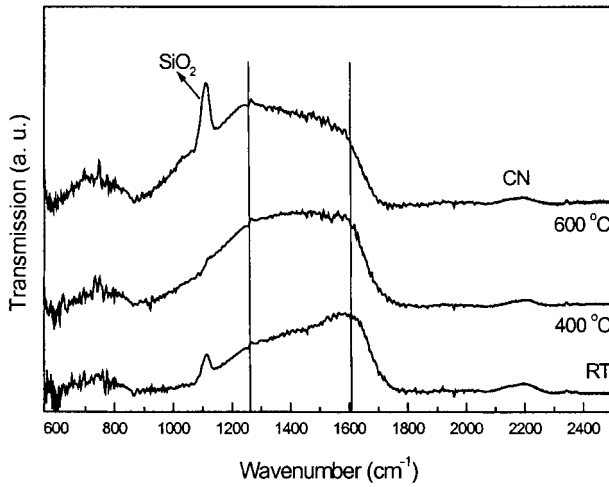
High substrate temperature is usually a drawback for the deposition of carbon films, because a transition from highly sp^3 to sp^2 bonded carbon occurs at temperatures above 200°C.¹⁷ However, in order to obtain diamond or cBN, substrate temperatures above 800°C are necessary.²⁰ In these cases, a high substrate temperature is necessary to give enough adatom mobility to allow the atoms to be accommodated in the appropriate lattice positions.

A common effect of high substrate temperatures in CN films is a decrease in the deposition rate and nitrogen incorporation. The composition of the sample at room temperature (RT) was 23.2 at.-%N and 27.7 at.-%H, as measured with ERDA-RBS. It has been reported in several papers that the nitrogen content decreases with increasing substrate temperature T_S .²¹ However, the effect is stronger for substrate temperatures above 600°C. The film composition (N and H at.-%) for the samples deposited at high substrate temperatures could not be measured during the period of this research. Nevertheless, film property variations are reported as a function of T_S , keeping in mind that the nitrogen content might be slightly decreasing.

The ta-C:N:H samples were deposited using a fixed N_2/C_2H_2 ratio of 2.5, equivalent to ~30% N_2 in the gas phase. The temperature was increased from RT to 600°C. Figure 8 confirms that there is a



8 Deposition rate as function of substrate temperature



9 Infrared spectra of ta-C:N:H samples deposited at different substrate temperatures

decrease in the deposition rate. This effect is related to an enhanced evolution of the volatile species, such as $(\text{CN})_n$ or HCN, but also a higher diffusion rate can easily increase the removal of N_2 molecules from within the sample.

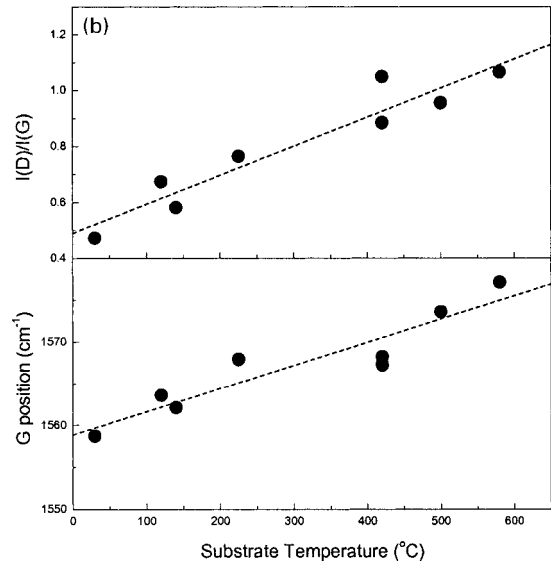
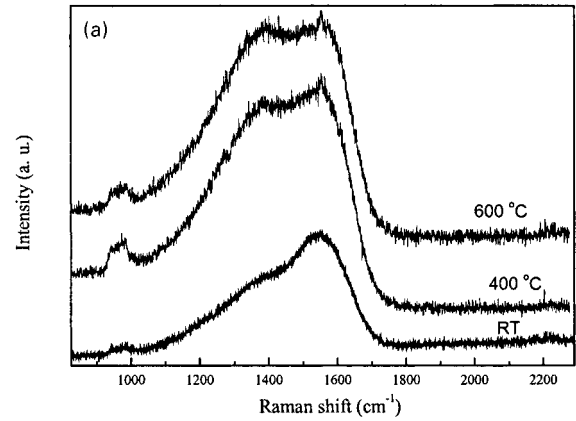
The evolution of the ir spectra and quite drastic changes in the $1000\text{--}1600\text{ cm}^{-1}$ region can be seen in Fig. 9. At RT, this band is asymmetrically towards 1600 cm^{-1} , as for many a-CNH samples, but as T_s is increased, the broad band becomes asymmetric to lower wavenumbers. Yap *et al.*³² observed similar changes for CN samples deposited by laser ablation at high substrate temperatures. He interpreted the increase in the 1300 cm^{-1} band as a rise in the fraction of CN single bonds. However, this is debatable, as there is considerable uncertainty in the assignment of this broad band.

The Raman spectra shown in Fig. 10a were fitted with a BWF function for the G peak and a Lorentzian for the D peak. The results of such a fitting are shown in Fig. 10b. The $I(D)/I(G)$ intensity ratio and the G position increase linearly with substrate temperature, indicating that the sp^2 sites are ordering into larger aromatic clusters.

The variation in the optical gap with substrate temperature is plotted in Fig. 11. The band gap declines gradually with T_s . The E_{04} drops from 1.6 eV to 0.7 eV for temperatures above 350°C and then remains unchanged.

Discussion of effect of substrate temperature

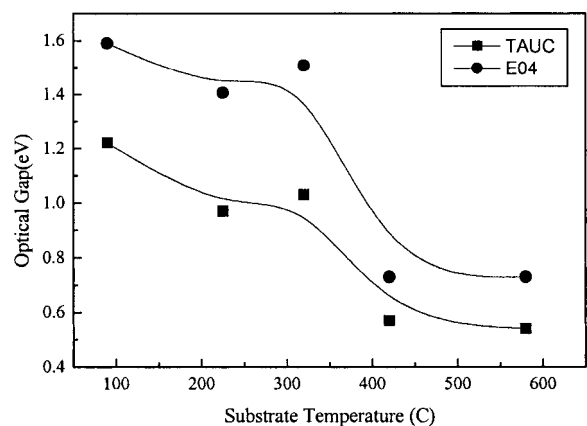
For ta-C:H films, Sattel *et al.*³³ showed that the film properties (percentage sp^3 , density and mechanical properties) present two transitions as functions of the deposition temperature: a lower transition $T_1 \sim 250^\circ\text{C}$ due to graphitisation of the C-C network and a second $T_2 \sim 400^\circ\text{C}$ due to a loss of bound hydrogen, while the band gap decreases gradually, even for temperatures below T_1 , in a similar way to that observed for ta-C films,¹⁸ where the films below T_1 are sp^3 bonded with gap decreasing gradually. Between T_1 and T_2 , they have a soft, disordered sp^2 structure with a gap $\sim 0.5\text{ eV}$. Above T_2 , the films are highly graphitic, where the gap has completely closed and a Raman spectrum is similar to nanocrystalline graphite; showing two sharp D and G peaks.



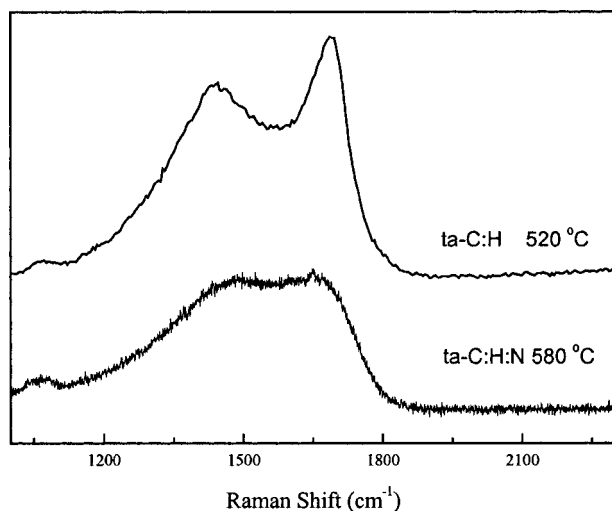
10 a Raman spectra of ta-C:N:H films deposited at different substrate temperatures; b Raman parameters v. substrate temperature

For the present samples, the variation in the Raman parameters and the optical gap correlate well. The substrate temperature provides the energy needed to gather the sp^2 sites into larger clusters. Therefore, the gap varies inversely with the cluster size, which increases as the substrate temperature increases, explaining the decrease in the gap.

For a carbon film, this behaviour suggests 'graphitisation' of the sample. The band gap shrinks, conductivity increases and the Raman spectra show an increasing $I(D)/I(G)$ ratio. However, Fig. 12 shows



11 Optical gap v. substrate temperature



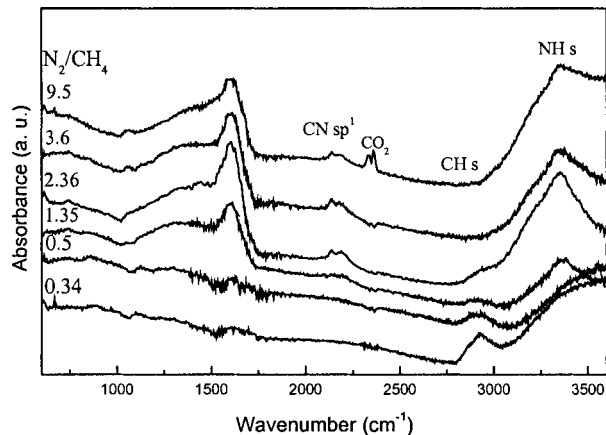
12 Raman spectra of ta-C:H sample deposited at 520°C compared with that of ta-C:N:H sample deposited at 580°C; narrow peaks are indication of ordering

that the Raman spectra of ta-C:H deposited at 520°C is quite different from that of ta-C:N:H deposited at a somewhat higher temperature. This is an indication that the presence of nitrogen in the samples inhibits graphitisation. In this case, graphitisation means the ordering of the graphene planes along the *c* axis. This figure shows clearly why the term graphitisation for CN films is incorrectly used, since nitrogen inhibits complete ordering of the graphene layers. This is probably because the presence of nitrogen in the structure tends to cause the graphene units to become curved.²²

There is no contradiction between the results of the previous section, where as the nitrogen content was increased, an ordering of the sp² sites was detected, and these results, in which even at high temperatures some disorder is still present. The previous section stated that at low nitrogen content, nitrogen induces the formation of sp² clusters, but at higher concentrations this tendency seems to cease as no further ordering is observed for N > 20 at.-%. This is most likely due to the low stability of the large plane structures. Similarly, with the increase in substrate temperature, ordering of the sp² sites is occurring, but as nitrogen is present, the graphene planes are interrupted by nitrogen atoms bonded to the edges or by crosslinking between the planes, limiting the degree of ordering needed to graphitise the sample.

Effect of hydrocarbon gas

It is important to ascertain the effects of plasma species variations on film properties. Therefore, optical emission spectra as a function of the nitrogen partial pressure were measured prior to deposition. The emission spectra of a pure acetylene plasma show emission lines superimposed on a broad background, which is attributed to electron transitions within the plasma.²³ The most intense absorption lines are those related to CH excited species at 390 and 430 nm and the H₂ at 655 nm. The CN band and all the nitrogen associated bands increase, while the CH bands decrease, as the N₂ partial pressure increases. This has a marked impact on the growth rate of the films, as shown in Fig. 1.

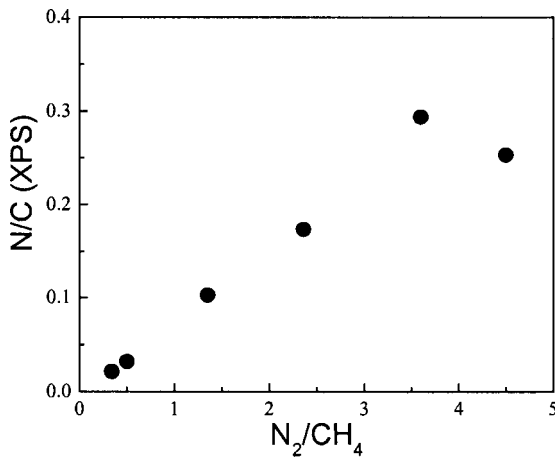


13 Infrared spectra of samples deposited with increasing N₂/CH₄ ratio

The emission intensity of methane plasmas is not obscured by an intense background as in the case of acetylene. Therefore, a more detailed study of the variation in the plasma species could be obtained in this case. The CH line at 428 nm is the most intense, and the intensity of the H₂ line relative to the CH line is larger than the case for acetylene.²⁴ As the N₂ partial pressure increases, there is an initial increase in the emission intensity of the nitrogen species, including CN, with a corresponding decrease in CH and H intensities. This is expected, because the concentration of N₂ molecules and, therefore their effective capture cross-section has increased. However, the fact that this is observed even at very low N₂ concentrations reflects the fact that nitrogen species are principally produced by primary electron excitation, whereas the CH_x species are generated through secondary collisional processes. The higher concentration of hydrogen in the gas phase induces a decay in the deposition rate sharper than that observed for acetylene samples (Fig. 1). It is interesting to note that the deposition rate decreases even when a higher fraction of CN species is observed in the gas phase, indicating that CN radicals are not the principal deposition precursor.

The ion energy was monitored with a Faraday cup, keeping the maximum value ~40–50 eV, because film growth was strongly inhibited at higher energies. The evolution of the ir spectra as the N₂/CH₄ was increased can be seen in Fig. 13. In this case, the samples were deposited on double sided polished silicon substrates to avoid the strong background seen in Fig. 4. At low ratios, only the CH stretching bands are observed (3000 cm⁻¹). However, when the ratio exceeds 1:3, new features are clearly detected: a broad asymmetric band ~1500 cm⁻¹ similar to the band in Fig. 13. The 2200 cm⁻¹ band is stronger than for the acetylene samples and has a double structure reflecting the presence of both C≡N and -N=C=N- groups. Finally, the CH stretching band decreases, whereas the NH stretching bands increase as previously observed for the acetylene samples.

Preliminary EELS results obtained from the C-K edge suggest a C sp³ fraction ~50–60% and plasmon energies ~26 eV. Figure 14 shows the results of the XPS analysis of the methane samples. It can be seen that the nitrogen content in the deposit is directly proportional to its concentration in the gas mixture.



14 Results of XPS elemental analysis of methane samples

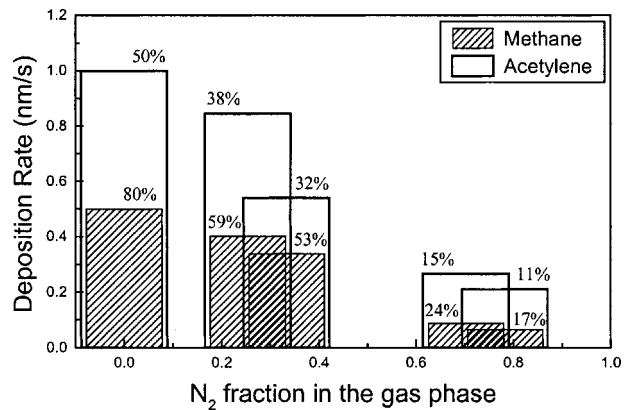
Discussion of effect of hydrocarbon gas

The main interest in depositing ta-C:N:H samples from a combination of either methane or acetylene mixed with nitrogen was to study the effect of a higher hydrogen fraction in both the gas phase and within the films. Hydrogen has been found to be an important factor for the synthesis of crystalline films, such as diamond and microcrystalline silicon. In these two cases, high hydrogen dilutions are critical in obtaining good quality crystals. In diamond growth, for example, hydrogen is multifunctional; it selectively etches the sp^2 bonded carbon, and stabilises the diamond surface, creating new growth sites on these surfaces by atomic hydrogen abstraction.²⁵

For amorphous carbon, hydrogen plays a different role. It is incorporated in the films and helps to stabilise the sp^3 carbon fraction by saturation of π bonds, converting C-C sp^2 sites into CH sp^3 sites. This affects the film properties. a-C:H films with a wide range of optical gaps, conductivity, refractive index and densities have been produced.²¹ The growth of a-C:H through the subplantation process is still effective, the hydrogen content and therefore the film properties are modified by the ion bombardment. However, this successful effect of hydrogen is not applicable in all cases. For example, the other superhard material cBN, whose growth also relies on ion bombardment, is hindered by the presence of hydrogen in the gas phase.²⁶ In this case, there is neither a selective etching of the hexagonal phase nor a stabilisation of the tetrahedral bonding.

Therefore, the effect of hydrogen in CN systems cannot be assumed from previous information. Recent calculations of gas phase reactions of hydrocarbon species with nitrogen hydride species at the molecular level suggest that hydrogen abstraction reactions that make the CVD deposition of diamond thin films successful do not favour the formation of CN thin films.²⁷ This is due to the formation of volatile HCN and CNH molecules by hydrogen abstraction processes which have negligible energy barriers and in some cases are exothermic.

Many attempts have been made to deposit CN films by CVD methods. A common outcome of these attempts is a low nitrogen content when compared with physical vapour deposition (PVD) methods. This latter statement is valid for the present work; the nitrogen content saturates ~ 30 at.-% for ta-C:N:H



15 Deposition rate decreases with N_2 partial pressure, but is lower for methane samples, since H_2 partial pressure is always higher; H_2 partial pressures are at top of each column

compared with 45 at.-% for the ta-C:N samples, suggesting that hydrogen induces lower nitrogen incorporation. This is in agreement with the results of Hammer.²⁸ He studied the effect of hydrogen on carbon nitride films deposited by ion beam assisted deposition, in which a graphite target was ablated by a nitrogen beam, while the growing film was simultaneously bombarded with N and H ions.

The other effect of increasing the hydrogen partial pressure is a decrease in the deposition rate. This is observed when comparing the deposition rates of the ta-C:N:H samples deposited with methane and acetylene (see Fig. 15).

In both cases, the deposition rate decreases with the nitrogen partial pressure, but comparing the rates for similar N_2 fractions, the methane samples always have lower values, as observed in Figs. 1 and 15.

The main difference between acetylene and methane is the higher hydrogen fraction in the methane gas. This is clearly observed in Hammer's work, with an 85% reduction in the deposition rate when the hydrogen partial pressure is increased to 70%. The effect is even more critical in dc magnetron sputtered samples, where the deposition rate goes to zero for hydrogen partial pressure of more than 15%.²⁹

The deposition rates and nitrogen incorporation clearly indicate that some chemical effects involving desorption of both nitrogen and carbon from the growing film occurs. The presence of hydrogen enhances this chemical sputtering by the formation of HCN or CNH species.

It is clear in Fig. 1 that the growth rate for the methane samples also decreases for samples prepared without nitrogen. In both a-C:H and a-C:N:H samples, hydrogen is incorporated within the films. However, in a-C:N:H samples, there is preferential NH bonding.³⁰ In general, this preferential NH bonding has been deduced from ir spectra, where the CH stretching band intensity decreases, while the NH stretching band intensity increases with the nitrogen concentration (see Figs. 4 and 13). Although this effect could also be explained by a higher ir cross-section for NH vibrations compared with CH modes, hydrogen effusion results confirmed the favoured NH bonding, since almost no hydrocarbons are found and mainly HCN is obtained.

Concerning the film properties, the implications of this NH bonding are strong. In a-C:H, the exothermic $[-C=C- + H_2 \Rightarrow CH-CH=]$ reaction promotes sp^3 bonding and also reduces the size of the sp^2 clusters. However, in a-C:N:H, this mechanism is lost, explaining to some extent the increase in cluster size at low nitrogen incorporation (Fig. 5c).

In ta-C:H, for example, there are $\sim 25-35\%$ sp^3 CH bonds.²⁸ When nitrogen is incorporated, this fraction decreases through the formation of $>C=NH$, $>C=N-NH_2$ or $C-NH_2$ bonds. According to the results obtained for the ta-C:N samples, the two first structures are more likely at high nitrogen concentrations, since CN bonds are most favoured.

In conclusion, the presence of hydrogen is detrimental for both the growth of carbon nitride and the formation of a high density amorphous C:N:H network.

CONCLUSIONS

On the one hand, the total nitrogen percentage increases with increasing nitrogen supply but gradually reaches a saturation value, independent of the ion energy and the type of hydrocarbon gas. The hydrogen content, on the other hand, decreases slightly as the percentage of nitrogen increases.

The optical gap, EELS and vibrational results suggest that, as the nitrogen content increases in the deposits, there is a transition to more polymeric films. The total hydrogen content does not change much, but the hydrogen transfers from bonding to sp^3 carbon sites to a preferential bonding in NH groups. This leaves the carbon in sp^2 sites, which leads to a lower optical gap. The mean coordination number of this latter network is much lower, such that the films can be scratched and are polymer-like in nature.

Alternatively, the effect of the ion energy is very similar to the substrate bias effect in the deposition of a-C:H samples in the range where the film changes from polymeric to diamond-like. The percentage of hydrogen and optical gap decrease slightly as a function of the ion energy (40–120 eV) while the mass density increases.

Although the composition of the films deposited at high substrate temperatures was not obtained, the variations in the optical gap and vibrational spectra suggest a decrease in hydrogen content and ordering of the sp^2 phase into larger clusters. This ordering is limited, however, by the presence of nitrogen.

Hydrogen is detrimental to the deposition of carbon nitride films. During the growth, it enhances the chemical etching effect of nitrogen species, most probably by forming HCN species, which are extremely volatile. Hydrogen incorporated within the films decreases the film density because it preferentially bonds to the nitrogen, forming terminating groups. Therefore, films deposited under these conditions are highly polymeric, exhibiting higher band gaps and sharper features in the ir spectra.

REFERENCES

1. M. L. COHEN: *Phys. Rev. B*, 1985, **32**, 7988.
2. M. L. COHEN: *Science*, 1993, **261**, 307.
3. S. MUHL and J. M. MÉNDEZ: *Diam. Relat. Mater.*, 1999, **8**, 1809–1830.
4. T. Y. YEN and C. P. CHOU: *Appl. Phys. Lett.*, 1995, **67**, 2801–2803.
5. L.-W. YIN, M.-S. LI, J.-L. SUI and J.-M. WANG: *Chem. Phys. Lett.*, 2003, **369**, 483.
6. S. R. P. SILVA, J. ROBERTSON, G. A. J. AMARATUNGA, B. RAFFERTY, L. M. BROWN, D. F. FRANCESCHINI and G. MARIOTTO: *J. Appl. Phys.*, 1997, **81**, 2626–2634.
7. G. FRANCHINI, A. TAGLIAFERRO and S. C. RAY: *Diam. Relat. Mater.*, 2003, **12**, 208–218.
8. S. BHATTACHARYYA, M. HIETSCHOLD and F. RICHTER: *Diam. Relat. Mater.*, 2000, **9**, 544–529.
9. S. E. RODIL, W. I. MILNE, J. ROBERTSON and L. M. BROWN: *Appl. Phys. Lett.*, 2000, **77**, 1458–1460.
10. M. LACERDA, M. LEJEUNE, B. J. JONES, R. C. BARKLIE, R. BOUZERAR, K. ZELOLAMA, N. M. J. CONWAY and C. GODET: *J. Non-Cryst. Solids*, 2002, **299–302**, 907–911.
11. S. E. RODIL, N. A. MORRISON, J. ROBERTSON and W. I. MILNE: *Phys. Status Solidi (a)*, 1999, **175**, 25–37.
12. M. WEILER, S. SATTEL, T. GIessen, K. JUNG and H. EHRHARDT: *Phys. Rev. B*, 1996, **53**, 1594.
13. N. A. MORRISON, S. MUHL, S. E. RODIL, A. C. FERRARI, M. NESLÁDEK, W. I. MILNE and J. ROBERTSON: *Phys. Status Solidi (a)*, 1999, **172**, 79–90.
14. N. P. BARRADAS, C. JEYNES, R. P. WEBB, U. KREISSIG and R. GRÖTZSCHEL: *Nucl. Instrum. Methods Phys. Res. B*, 1999, **149**, 233.
15. S. E. RODIL, N. A. MORRISON, W. I. MILNE, J. R. ROBERTSON, V. STOLOJAN and D. N. JAYAWARDANE: *Diam. Relat. Mater.*, 2000, **9**, 524–529.
16. S. E. RODIL, A. C. FERRARI, J. ROBERTSON and S. MUHL: *Thin Solid Films*, 2002, **420–421**, 122–131.
17. A. C. FERRARI, S. E. RODIL and J. ROBERTSON: *Phys. Rev. B*, 2003, **67**, 155306-1–155306-20.
18. S. E. RODIL, A. C. FERRARI, J. ROBERTSON and W. I. MILNE: *J. Appl. Phys.*, 2001, **89**, 5425–5430.
19. A. MARCHON, J. GUI, K. GRANNEN, G. C. RAUCH, J. W. AGER, S. R. P. SILVA and J. ROBERTSON: *IEEE Trans. Mag.*, 1997, **76**, 335.
20. M. CHHOWALLA, A. C. FERRARI, J. ROBERTSON and G. A. J. AMARATUNGA: *Appl. Phys. Lett.*, 2000, **76**, 1.
21. W. KULISCH: 'Deposition of diamond-like superhard material'; 1999, Berlin, Springer.
22. H. SJÖSTRÖM, L. HULTMAN, J. E. SUNDGREN, S. V. HAINSWORTH, T. F. PAGE and G. S. A. M. THEUNISSEN: *J. Vac. Sci. Technol. A*, 1996, **14**, 56–62.
23. N. HELLGREN, M. P. JOHANSSON, E. BROITMAN, L. HULTMAN and J. E. SUNDGREN: *Appl. Phys. Lett.*, 2001, **78**, 2703–2705.
24. A. R. GRIEM: 'Plasma spectroscopy'; 1964, New York, McGraw-Hill.
25. N. M. J. CONWAY: PhD thesis, University of Cambridge, 1998.
26. J. ROBERTSON: *Materials Sci. Eng. R*, 2002, **37**, 129–281.
27. J. L. ANDUJAR, E. BERTRAN and M. C. POLO: *J. Vac. Sci. Technol. A*, 1998, **16**, 578.
28. P. HAMMER, N. M. VICTORIA and F. ALVAREZ: *J. Vac. Sci. Technol. A*, 1998, **16**, 2941–2949.
29. R. Q. ZHANG, K. L. HAN, R. S. ZHU, C. S. LEE and S. T. LEE: *Chem. Phys. Lett.*, 2000, **321**, 101.
30. N. HELLGREN, M. P. JOHANSSON, B. HJORVARSSON, E. BROITMAN, M. OSTBLOM, B. LIEBERG, L. HULTMAN and J. E. SUNDGREN: *J. Vac. Sci. Technol. A*, 2000, **18**, 2349.
31. N. MUTSUKURA and K. AKITA: *Diam. Relat. Mater.*, 1999, **8**, 1720.
32. Y. K. YAP, S. KIDA, T. AOYAMA, Y. MORI and T. SASAKI: *Appl. Phys. Lett.*, 1998, **73**, 915.
33. S. SATTEL, J. ROBERTSON and H. EHRHARDT: *J. Appl. Phys.*, 1997, **82**, 4566.